

Supplementary Information for: Phase Diagram of ZIF-4 from Computer Simulations

Emilio Méndez, Rocio Semino

Sorbonne Université, CNRS, Physico-chimie des Electrolytes et
Nanosystèmes Interfaciaux, PHENIX, F-75005 Paris, France
E-mail: rocio.semino@sorbonne-universite.fr

Simulation details

We performed all simulations via the LAMMPS open source software[7], coupled with the PLUMED[9] package for implementing well-tempered metadynamics. The nb-ZIF-FF force field was used to model the interactions[1]. This force field has two main features: (i) the inclusion of dummy atoms in Zn^{2+} and N (within imidazole) species to correctly reproduce the tetrahedral coordination environment around the metal, and (ii) the possibility of metal-ligand bond breaking/formation through the use of non bonded interaction terms in the form of Morse potentials. This force field is also known to reproduce the experimental properties of several ZIF polymorphs including ZIF-4, along with the corresponding glasses obtained through ambient pressure thermal amorphization.[1, 4] Bonded terms are based on the ZIF-FF force field[10] and include harmonic style bonds, harmonic plus an additional Urey Bradley term for angles and cosine based dihedrals and impropers. Coulombic interactions are computed via the particle-particle/particle-mesh method while all dispersion interactions (Morse potentials for coordination bonds and 12-6 Lennard-Jones for the rest of the species) were computed considering a cutoff of 1.3 nm.

The integration of the equations of motion was done in the NPT ensemble, using Nose-Hoover thermostats and barostats [3]. The temperature was set to 300 K, and the damping parameters were set to 100 and 1000 time steps for regulating temperature and pressure respectively. The barostat acted independently in each of the three system dimensions to allow the cell

parameters to evolve in an unconstrained way. In all cases the simulation box was kept orthorhombic.

The parameters for well-tempered metadynamics were 9 kJ/mol and 0.1 nm for the initial gaussian height and standard deviation, respectively, and 75 for the bias factor that controls the decay of the heights with time. Five parallel walkers were employed to accelerate the metadynamics convergence.[6] Each walker evolves independently from the others but they all share the same bias potential obtained from the addition of gaussian terms. The time step was set to 0.5 fs and the total time for each simulation, comprising all the walkers, was around 100 ns. Additional constraints were included for preventing the system from exploring non physical regions. These consisted in upper and lower bounds for each of the cell parameters and for the total volume, as well as a lower bound for the Zn-N total coordination to avoid metal-ligand bond breaking events that could lead to amorphization. This is because no amorphous phase has been experimentally reported in the phase diagram region that we target for exploration in this work. As a consequence, all the studied phases retained the connectivity of ZIF-4, resulting in a tetra-coordination for all the Zn^{2+} in the simulation box.

Metadynamics simulations were conducted at 0, 40 and 80 MPa. All of them started from a 2x2x2 super cell of ZIF-4, which contains a total of 128 Zn^{2+} atoms and has dimensions of 3.08x3.06x3.68 nm³. Additionally, a few unbiased molecular dynamics simulations were performed for each of the obtained polymorphs. These were all carried out in the NPT ensemble for the thermodynamic conditions specified in each case, with the same force field, thermostat, barostat and timestep as those reported for the well-tempered metadynamics.

Well-tempered Metadynamics Setup

The following script was used as PLUMED input file for the configuration of the well-tempered metadynamics runs:

```
1 # Define volume and cell parameters:
2 vol: VOLUME
3 cell: CELL
4
5 # Read Zn and N atom indexes from ndx file:
6 Zn_atoms: GROUP NDX_FILE=index.ndx NDX_GROUP=zn
7 N_atoms: GROUP NDX_FILE=index.ndx NDX_GROUP=n
8
9 # Calculate the Zn-N coordination number:
10 cn: COORDINATION GROUPA=Zn_atoms GROUPB=N_atoms R_0=0.05 D_0=0.22 NN=6
11
```

```

12 # Metadynamics setup:
13 meta: METAD ...
14 ARG=cell.ax,cell.by,cell.cz
15 SIGMA=0.1,0.1,0.1
16 HEIGHT=9.0
17 BIASFACTOR=75.0
18 TEMP=300.0
19 PACE=1000
20 GRID_MIN=2.4,2.4,2.4
21 GRID_MAX=4.4,4.4,4.4
22 GRID_BIN=200,200,200
23 WALKERS_N=5
24 WALKERS_ID=0
25 WALKERS_DIR=./
26 WALKERS_RSTRIDE=1000
27 ...
28
29 # Additional constraints:
30 uwall: UPPER_WALLS ARG=vol,cell.ax,cell.by,cell.cz AT=36.0,3.8,3.8,3.8 KAPPA
    =10000,50000,50000,50000 EXP=2,2,2,2
31 lwall: LOWER_WALLS ARG=vol,cell.ax,cell.by,cell.cz,cn AT=16.0,2.6,2.6,2.6,511.0
    KAPPA=10000,50000,50000,50000,50000 EXP=2,2,2,2,2
32
33 # Output:
34 PRINT ARG=vol,cell.ax,cell.by,cell.cz,uwall.bias,lwall.bias,meta.bias,cn FILE=colva
    .dat STRIDE=1000

```

Each section contains a comment explaining the aim of the code fragment that follows. Default PLUMED units were used: nm for distance, ps for time and kJ/mol for energy. The cell parameters a , b and c are called 'cell.ax', 'cell.by' and 'cell.cz'. The coordination number command 'COORDINATION' counts the number of Zn-N pairs at a distance lower than 0.22 nm, a slightly higher value than the typical bond length of 0.21 nm. This number is constrained through the 'LOWER_WALLS' command to be always higher than 511. Since the total coordination number in the system is 512, this prevents Zn-ligand bond breaking events. Additional descriptions of each command can be found in the PLUMED manual.

Metadynamics Convergence and Data Treatment

To check if the order parameter space was correctly sampled during the simulation, we plotted the evolution of a , b and c over time in Fig. 1, for the simulation at $P = 40$ MPa. These results include the data from the five walkers of the metadynamics. Although it is not possible to directly assign each point to one of the studied polymorphs to observe the presence of interconversion events due to the high dimensionality of the order parameter space, it is clear that virtually all the points in the accessible region were

visited multiple times, which is a necessary condition for the convergence of the method. Similar results were obtained for the simulations at $P = 0$ and 80 MPa.

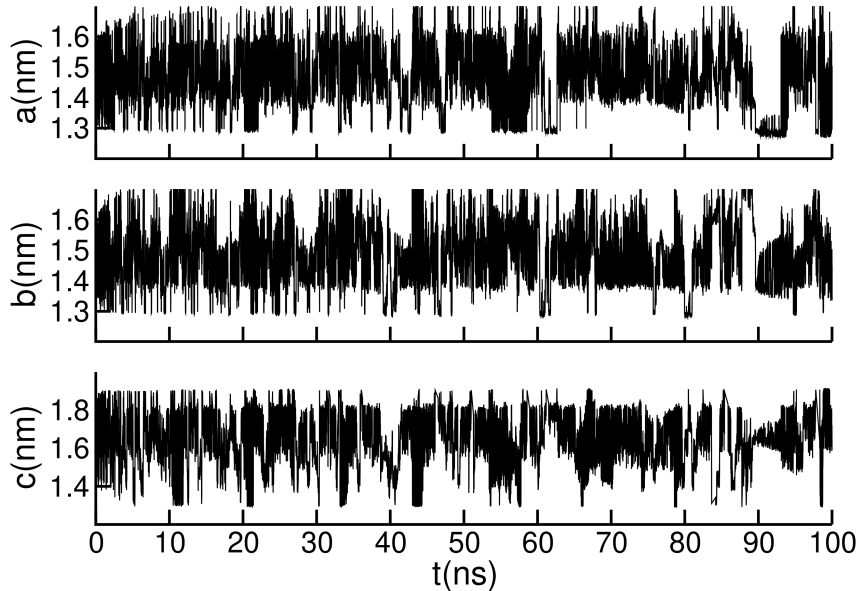


Figure 1: Collective variables a , b , and c as a function of time for the $P = 40$ MPa simulation. Results from all the five walkers are concatenated.

To analyze the convergence of the well-tempered metadynamics simulations we followed the procedure developed by Tiwary et al.[8] This approach takes into account the fact that in metadynamics the bias potential is dynamically modified as the simulation advances, never reaching a plateau value. This makes the choice of a convergence criterion a non trivial task. The authors found a way to compute a time independent free energy estimator that allows to compare results measured at different times during the simulation given by:

$$G(s) = -\frac{\gamma V(s, t)}{(\gamma - 1)} + k_b T \ln \int e^{\frac{\gamma V(s, t)}{(\gamma - 1) k_b T}} ds \quad (1)$$

where s represents the collective variable(s), γ the bias factor, and $V(s, t)$ the time dependent bias potential. The last term is a time dependent constant that aligns the free energy estimation at time t with the ones computed at previous times. For applying this technique to data obtained from different walkers, we time-ordered the gaussians coming from each simulation. In Fig.

2 we plotted the free energy estimator $G(a, b, c)$ of eq. 1 as a function of time for three (a, b, c) points that roughly correspond to the lattice constants of the studied polymorphs. We also plotted the free energy without the addition of the second term of eq. (1). As expected, these last values continue to descend without reaching a plateau, but the corrected estimators fluctuate around fixed values.

In order to compute the final free energy profile and the corresponding errors, we need to time average the results from the corrected free energy curves. To avoid artifacts that arise when dealing with correlated data, we employed the block averaging technique developed by Bussi and Tribello.[2] To estimate the optimal block size for which the data is uncorrelated, we computed the standard deviation of the free energy as a function of the block size. The results are shown in figure 3 for the (a, b, c) point that corresponds to the lowest minimum. When the individual block values become uncorrelated, the standard deviation reaches a plateau. According to this criterion, we averaged data from blocks of 8 ns.

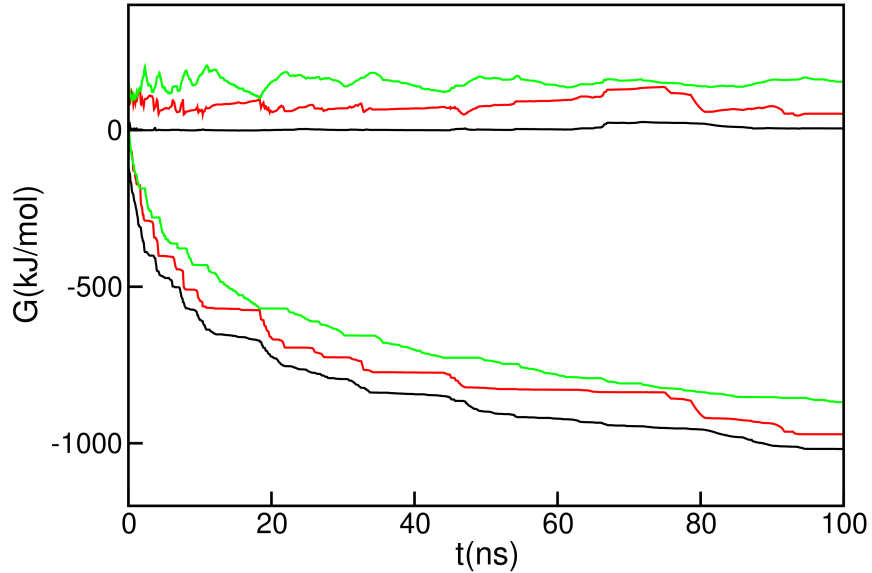


Figure 2: Free energy estimator for points in the (a, b, c) space that corresponds to ZIF-4 (green), ZIF-4-cp (black) and ZIF-4-cp-II (red) lattice constants for the simulation at $P = 40$ MPa. The curves in the negative region correspond to the estimator without the correction term of Eq. (1).

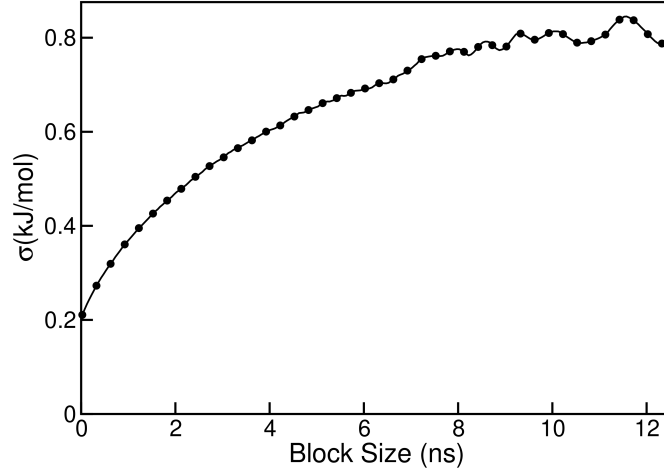


Figure 3: Free energy standard deviation for the absolute minimum as a function of the block size.

Multitermal Multibarcic Ensemble

In the multitermal multibarcic ensemble developed by Piaggi et. al,[5] a metadynamics simulation is performed with the energy E and volume V as order parameters. In this context the authors derive an expression that links the free energy at pressure P and temperature T , $G^{(T,P)}(E, V)$, with the one corresponding to a thermodynamic state (T', P') from statistical mechanics considerations:

$$\beta' G^{(T',P')}(E, V) = \beta G^{(T,P)}(E, V) + (\beta' - \beta)E + (\beta'P' - \beta P)V + C \quad (2)$$

where $\beta = 1/k_bT$, $\beta' = 1/k_bT'$, and C is a constant that does not depend on E and V . Since we aimed to study the properties of the polymorphs at different pressure conditions but at constant temperature, we did not bias the energy. For an isotherm, equation (2) simplifies to:

$$G^{(P')}(V) = G^{(P)}(V) + (P' - P)V + C \quad (3)$$

Finally, if the order parameters are the cell dimensions instead of the volume, equation (3) trivially turns into:

$$G^{(P')}(a, b, c) = G^{(P)}(a, b, c) + (P' - P)V + C \quad (4)$$

where a , b and c are the dimensions of the simulation box in the x , y and z directions respectively, and $V = a.b.c$ since we only considered orthorhombic configurations.

Calculation of $G(V)$

For the computation of the free energy as a function of the volume at pressure P ($G^{(P)}(V)$) starting from the function $G^{(P)}(a, b, c)$ that was obtained from the well-tempered metadynamics simulations, we proceeded as follows. First, we computed the probability $\mathcal{P}^{(P)}(a, b, c)$ given by the Boltzmann distribution:

$$\mathcal{P}^{(P)}(a, b, c) = C' e^{-\beta G^{(P)}(a, b, c)} \quad (5)$$

where C' is a normalization constant. Then, since the volume is an explicit function of a , b and c , the probability of the system to have volume V at a pressure P was obtained by the following integration:

$$\mathcal{P}^{(P)}(V) = \int \delta(V - abc) \mathcal{P}^{(P)}(a, b, c) da db dc \quad (6)$$

where $\delta(x)$ is the Dirac delta function. In practice, this integral was performed by discretizing the volume variable into bins. Finally $G(V)$ was obtained by the inversion of equation (5), now with the volume as variable:

$$G^{(P)}(V) = -1/\beta \ln \mathcal{P}^{(P)}(V) \quad (7)$$

The corresponding error bars were calculated by propagation of errors from equations (5), (6) and (7).

Additional Results

Table 1: Average angle between the normal vector to the 4-membered ring plane and each of the axes **a**, **b** and **c** in ZIF-4-cp and ZIF-4-cp-II. Experimental results computed from the available cif files are shown between parenthesis.

	ZIF-4-cp	ZIF-4-cp-II
a	52.3 (53.1)	48.7 (48.8)
b	41.9 (40.2)	44.0 (44.0)
c	74.7 (76.3)	77.6 (77.2)

References

- [1] S. R. G. Balestra and R. Semino. Computer simulation of the early stages of self-assembly and thermal decomposition of ZIF-8. *The Journal of Chemical Physics*, 157(18):184502, Nov. 2022.
- [2] G. Bussi and G. A. Tribello. *Analyzing and Biasing Simulations with PLUMED*. Springer New York, 2019.
- [3] D. J. Evans and B. L. Holian. The nose–hoover thermostat. *The Journal of Chemical Physics*, 83(8):4069–4074, Oct. 1985.
- [4] E. Méndez and R. Semino. Microscopic mechanism of thermal amorphization of zif-4 and melting of zif-zni revealed via molecular dynamics and machine learning techniques. *Journal of Materials Chemistry A*, 12(8):4572–4582, 2024.
- [5] P. M. Piaggi and M. Parrinello. Calculation of phase diagrams in the multithermal-multibaric ensemble. *The Journal of Chemical Physics*, 150(24):244119, June 2019.
- [6] P. Raiteri, A. Laio, F. L. Gervasio, C. Micheletti, and M. Parrinello. Efficient reconstruction of complex free energy landscapes by multiple walkers metadynamics. *The Journal of Physical Chemistry B*, 110(8):3533–3539, Oct. 2005.
- [7] A. P. Thompson, H. M. Aktulga, R. Berger, D. S. Bolintineanu, W. M. Brown, P. S. Crozier, P. J. in 't Veld, A. Kohlmeyer, S. G. Moore, T. D. Nguyen, R. Shan, M. J. Stevens, J. Tranchida, C. Trott, and S. J. Plimpton. LAMMPS - a flexible simulation tool for particle-based materials modeling at the atomic, meso, and continuum scales. *Computer Physics Communications*, 271:108171, Feb. 2022.
- [8] P. Tiwary and M. Parrinello. A time-independent free energy estimator for metadynamics. *The Journal of Physical Chemistry B*, 119(3):736–742, July 2014.
- [9] G. A. Tribello, M. Bonomi, D. Branduardi, C. Camilloni, and G. Bussi. Plumed 2: New feathers for an old bird. *Computer Physics Communications*, 185(2):604–613, Feb. 2014.
- [10] T. Weng and J. R. Schmidt. Flexible and transferable ab initio force field for zeolitic imidazolate frameworks: Zif-ff. *The Journal of Physical Chemistry A*, 123(13):3000–3012, Mar. 2019.